

Crystal Structures of Human Factor Xa Complexed with Potent Inhibitors

Sébastien Maignan,[†] Jean-Pierre Guilloteau,[†] Stéphanie Pouzieux,[†] Yong Mi Choi-Sledeski,[‡] Michael R. Becker,[‡] Scott I. Klein,[‡] William R. Ewing,[‡] Henry W. Pauls,[‡] Alfred P. Spada,[‡] and Vincent Mikol^{*†}

Department of Structural Biology, Aventis Pharma, 13, Quai J. Guesde, F-94403 Vitry/Seine, France, and
Department of Medicinal Chemistry, Aventis Pharma, 500 Arcola Road, Collegeville, Pennsylvania 19426

Received March 14, 2000

Involved in the coagulation cascade, factor Xa (FXa) is a serine protease which has received great interest as a potential target for the development of new antithrombotics. Although there is a great wealth of structural data on thrombin complexes, few structures of ligand/FXa complexes have been reported, presumably because of the difficulty in growing crystals. Reproducible crystallization conditions for human des-Gla1–45 coagulation FXa have been found. This has led to an improvement in the diffraction quality of the crystals (about 2.1 Å) when compared to the previously reported forms (2.3–2.8 Å) thus providing a suitable platform for a structure-based drug design approach. A series of crystal structures of noncovalent inhibitors complexed with FXa have been determined, three of which are presented herein. These include compounds containing the benzamidine moiety and surrogates of the basic group. The benzamidine-containing compound binds in a canonical fashion typical of synthetic serine protease inhibitors. On the contrary, molecules that contain surrogates of the benzamidine group do not make direct hydrogen-bonding interactions with the carboxylate of Asp189 at the bottom of the S1 pocket. The structural data provide a likely explanation for the specificity of these inhibitors and a great aid in the design of bioavailable potent FXa inhibitors.

Introduction

The serine protease factor Xa (FXa) is a key enzyme in the cascade-like activation of the coagulation system. It converts prothrombin to thrombin and holds a central position linking the extrinsic and intrinsic activation pathways. Compared to thrombin, FXa acts at an earlier step in the coagulation system and is not such a multifunctional protein.¹ Due to the amplification nature of the coagulation cascade, a small amount of FXa produces a large amount of thrombin, leading to the hypothesis that inhibition of FXa may be more efficient than inhibition of thrombin. In addition, it is anticipated that specific FXa inhibitors would prevent thrombus formation without compromising hemostasis as observed with thrombin inhibitors thus providing a better safety/efficacy profile.² This qualifies FXa as an attractive target for the development of new anticoagulant/anti-thrombotic drugs which may be advantageous over warfarin, heparin, low-molecular-weight heparins,³ and thrombin inhibitors for prophylaxis and/or treatment of thromboembolic disorders.

The three-dimensional crystal structure of FXa lacking the Gla (γ -carboxyglutamic acid) domain (45 N-terminal residues) has been solved free⁴ and complexed with potent arylamidine-containing inhibitors.^{5,6} They reveal that the inhibitors bind in an extended conformation with two main interaction sites made up by an ionic S1 pocket and by a hydrophobic S4 pocket. In contrast to the thrombin binding mode, the S2 site is not accessible providing scope for designing FXa-specific inhibitors. There is a great wealth of structural infor-

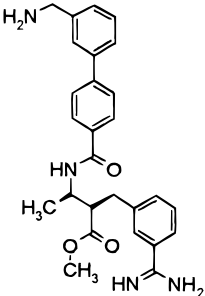
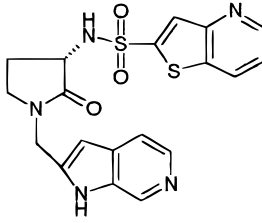
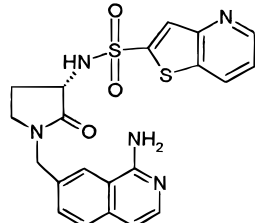
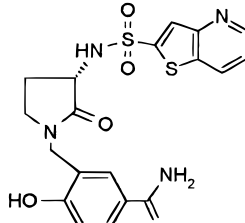
mation on thrombin/ligand complexes which has been critical for the design of specific inhibitors.⁷ Despite the strong interest in obtaining structural information, there have been to date very few reports on FXa/ligand complex structures, presumably because of the difficulty in growing crystals. To gain insight into the binding and conformation of bound FXa inhibitors, several groups have then determined bovine trypsin complexes.^{8,9} In this paper, we report reproducible crystallization conditions for human des-Gla1–45 coagulation FXa. This has led to an improvement in the diffraction quality of the crystals (about 2.1 Å) when compared to the previously reported forms (2.8–2.3 Å) thus providing a suitable platform for a structure-based drug design approach. A series of crystal structures of inhibitors complexed with FXa have been determined, three of which are presented herein (Table 1). These include compounds containing a benzamidine moiety and surrogates of the basic group. Compound **1** is a dibasic representative of the β -amino ester series¹⁰ which incorporates a benzamidine group as a P1 fragment and an aminomethyl-biphenyl group in the P4 position. This class of compounds exhibits potent affinity for FXa and high selectivity against other serine proteases, namely bovine β -trypsin (trypsin) and human thrombin. The usefulness of sulfonamidopyrrolidinone as a central template for the presentation of ligands to the S1 and S4 subsites has been recognized,¹¹ and studies to optimize the P1 and P4 groups were undertaken which has led to the preparation of compounds **2–4**. The crystal structures reported herein show that the P1 groups in compounds **1–3** appear to interact with the S1 pocket in different ways indicating that the formation of a salt bridge with the carboxylate of the bottom of the pocket is not an absolute requirement to maintain significant FXa af-

* Corresponding author: V. Mikol. Tel: 33 15571 3093. Fax: 33 15571 8063. E-mail: vincent.mikol@aventis.com.

[†] Aventis Pharma, France.

[‡] Aventis Pharma, Pennsylvania.

Table 1. Structures of FXa Inhibitors **1** (RPR128515), **2** (RPR208707), **3** (RPR208815), and **4** (RPR131247)^a

	1	2	3	4
structure				
K_i (FXa) (nM)	0.9	18	22	0.7
K_i (trypsin) (nM)	69	>2900	>2900	1000
K_i (thrombin) (nM)	>3000	>4000	>4000	>4000

^a The K_i values for FXa, bovine trypsin, and human thrombin are given for each compound. They were determined as previously described.²⁰

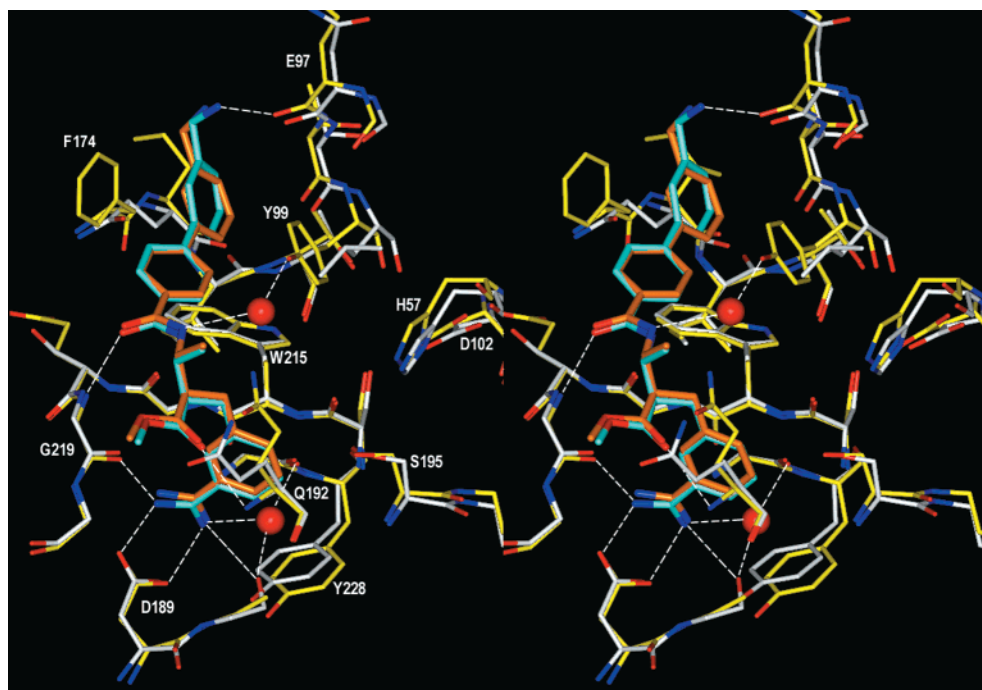


Figure 1. Binding interactions of **1** to FXa and trypsin. The residues from the proteins defining the binding site are displayed with thin lines and with nitrogen and oxygen atoms displayed in blue and red, respectively. Carbon atoms from FXa and trypsin are shown in yellow and white, respectively. Compound **1** is shown in thick lines with nitrogen and oxygen atoms displayed in blue and red, respectively. Carbon atoms of compound **1** bound to FXa and trypsin are shown in light blue and orange, respectively. H-bonds between **1** and FXa are indicated by dotted lines. Red balls represent water molecules as observed in the FXa/**1** complex. Overlay was made with the backbone atoms of the FXa and trypsin lying within 5 Å from **1**. Labels are given for FXa residues. Molecules are displayed with the same color code in all figures.

finity. The mode of interaction of these inhibitors with FXa will be described and compared with that observed in the trypsin crystal complexes. The structural data provide a likely explanation for the specificity of these inhibitors and are a great aid in the design of bioavailable FXa inhibitors.

Results

Conformation of the Protein. The overall structure of FXa does not undergo any major conformational rearrangement upon binding of the inhibitors, as indicated by the rmsd of 0.6 Å on 221 C α atoms between free and compound **1**-bound protein. Significant changes are only observed around the S4 site. As illustrated in Figure 1 the S4 pocket looks like a deep groove lined

by Y99, F174, and W215 on three sides. The plane of the aromatic rings of F174 and Y99 are almost parallel and lie perpendicular to that of W215. Upon binding to the protein, these residues close down on the ligand and constrict the S4 pocket. When compared with the apoenzyme the side chain atoms from both residues have moved toward the interior of the S4 cleft by about 1 Å to sandwich the P4 moiety of compound **1**.

Binding Mode of Inhibitors to FXa and Trypsin.

A. RPR128515 (1). FXa: Compound **1** displays excellent electron density and binds to FXa in an extended conformation with its benzamidine group located in the S1 pocket and the aminomethylbiphenyl group in the S4 pocket (Figure 1). The inhibitor does not interact with any residue of the S2 pocket. The benzamidine sits

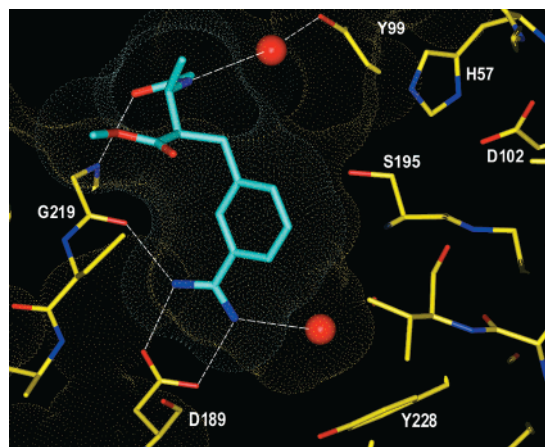


Figure 2. Close-up on the Connolly surfaces of **1** bound (light blue dots) to FXa (yellow dots).

in the S1 pocket and is involved in a salt bridge interaction with D189 (Figure 2). There is also a direct H-bond to the G219 carbonyl oxygen atom and a water-mediated H-bond to the I227 carbonyl oxygen atom. The ester group points opposite to the S2 site sitting on the C191–C220 disulfide bridge forming an H-bond with the Q192 main chain nitrogen. It fits snugly into a pocket made up by E147, Q192, G218, C191, and C220. This cleft appears relatively specific to FXa. The ester represents about 7% of the total buried area of the inhibitor upon binding. The amide nitrogen is engaged in a water-mediated H-bond with the Y99 hydroxyl group, and the amide carbonyl oxygen is involved in an H-bond with the G219 nitrogen. In addition, the carbonyl oxygen of **1** closely approaches the carbonyl oxygen of G216 (3.1 Å). This apparently unfavorable contact may be partially compensated by the close proximity of the NH of G219 to the carbonyl oxygen of the inhibitor. van der Waals contacts are made between the three aromatic residues (Y99, F174, and W215) from FXa and **1** providing a fit resembling a cylinder held by the jaws of flat-nose pliers (Y99 and F174) covered perpendicularly on one side by W215. There is an edge-to-face interaction between the terminal phenyl group and the indole side chain of W215 as typified by a centroid-to-centroid distance of 4.8 Å and a 79° inter-ring angle. This stabilization enables the establishment of a very strong H-bond between the amine group and the E97 carbonyl oxygen (distance of 2.5 Å and continuous electron density).

Trypsin: Compound **1** also adopts an extended conformation in the trypsin active site, and it is involved in a network of interactions very similar to that observed with FXa, typical of a synthetic inhibitor complexed with a serine protease (Figure 1). The only differences are found in the S1 and S4 pockets. In the S1 pocket, the substitution of S190 in trypsin by an alanine in FXa has induced an enlargement of the S1 site. S190 is involved in a direct H-bond with one of the amidine nitrogens. In the S4 pocket L99, Q175, and W215 play the role of the “wall” residues in trypsin, and van der Waals contacts are made between these three residues and the biphenyl group from **1** (Figure 1). The amino group attached to the biphenyl lies within H-bond distance (3.2 Å) from the N97 carbonyl oxygen. However this basic group shows some high mobility (high tem-

perature factor) and ill-defined electron density suggestive of a very loose contact. Amino acids L99 and Q175 from trypsin are substituted by two aromatic residues (Y99 and F174) in FXa. This renders the S4 groove deeper in FXa and increases its aromatic character. It allows for a better fit of the biphenyl where the second phenyl group is stacked between Y99 and F174 and forms an edge-to-face interaction with the indole side chain of W215. There is a gain of about 20% of contact surface when compared with trypsin. The aromatic stacking orients differently the second ring of the inhibitor in the FXa structure than in Trypsin ($\Delta = 20^\circ$). In this conformation the aminomethyl in FXa is situated in an ideal position to establish a strong H-bond with the E97 carbonyl oxygen.

The 70-fold difference in K_i between trypsin and FXa can presumably be accounted for by the structural data. It should be kept in mind that the simple molecule benzamidine shows a K_i of 100 μM against FXa and 35 μM against trypsin, suggesting that the overall energy gain (3-fold) resulting from the formation of the H-bond between a benzamidine-containing compound and the S190 hydroxyl group is rather limited. The weaker inhibition potency against trypsin when compared with FXa likely stems from more unfavorable contacts in the S4 pocket (no aromatic stacking, shallow groove with a contact surface reduced by 20%, looser H-bond, and absence of good complementarity in the “ester” pocket). This would suggest that significant specificity for FXa can be achieved by incorporating aromatic groups in the P4 position and/or occupying the “ester” pocket.

B. RPR208707 (2). As for **1**, compound **2** also binds in an extended conformation with the azaindole occupying the S1 pocket and the thienopyridine in the S4 pocket (Figure 3). The azaindole of **2** sits in the S1 pocket but is less buried by 1.5 Å when compared with the benzamidine equivalent of compound **1**. The pyridine moiety is not involved in direct electrostatic interaction with D189 but through a water-mediated contact. The pyrrolopyridine in **2** is expected to have pK_a value of 7.3 suggesting that under the crystallization conditions (pH = 5.7) the pyridine is protonated and could donate a hydrogen bond to D189. The pyrrolo nitrogen makes an H-bond with the G219 carbonyl oxygen atom, and the pyridine nitrogen is engaged in a water-mediated H-bond with D189. The carbonyl oxygen of the pyrrolidinone forms an H-bond with the G219 nitrogen, and the sulfonamide does not interact with the protein via any electrostatic interactions but makes some van der Waals contact with the enzyme. The thienopyridine group fits well in the S4 pocket stacked by the aromatic rings of Y99 and F174, and the pyridine moiety is involved in an edge-to-face contact with the indole of W125. The sulfur atom points toward the protein, and the pyridine nitrogen faces out toward the solvent and does not interact with the protein.

C. RPR208815 (3). The calculated pK_a of the aminoisoquinoline is estimated at about 7.6, indicating that the protonated form predominates under the crystallization conditions at pH 5.7 and that it could interact productively with D189 from the S1 subsite. However, no salt bridge is found for compound **3** between the aminoisoquinoline moiety and the carboxylate of D189 (distance of 3.7 Å between one of the carboxylate

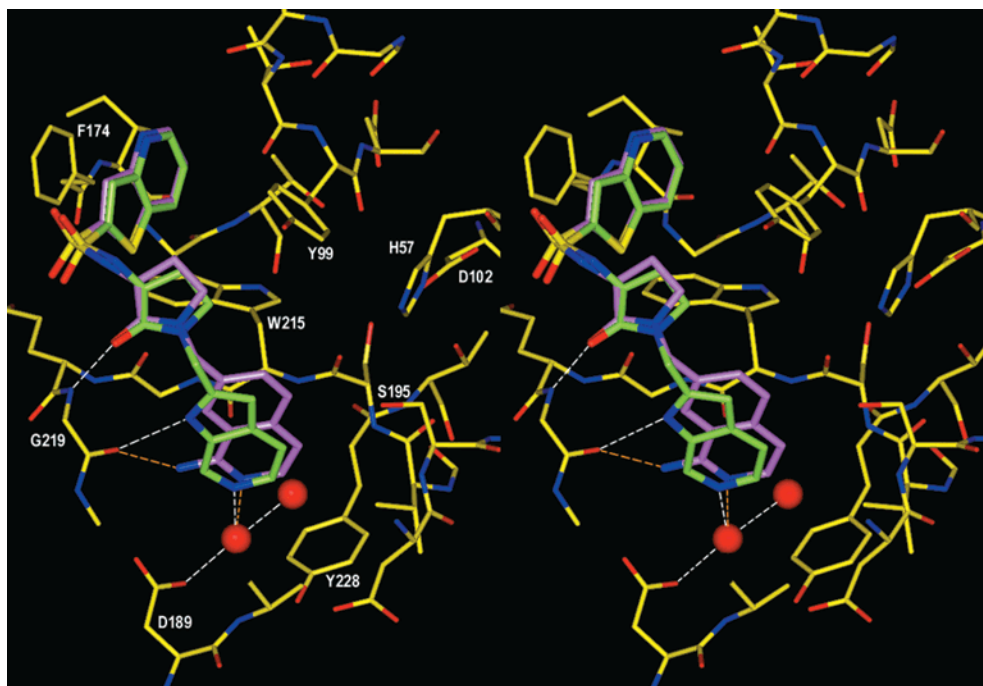


Figure 3. Binding interactions of **2** and **3** to FXa. **2** and **3** are shown in thick lines with carbons displayed in cyan and purple, respectively. H-bonds are indicated by white and orange dotted lines for FXa complexed with **2** and **3**, respectively.

oxygens and the amino group), but instead a water-mediated contact is observed (Figure 3). In addition to this solvent-bridging contact the other electrostatic interactions found in the S1 pocket include the H-bond between the carbonyl oxygen of G219 and the amino group of quinoline and a water-mediated contact between the amino nitrogen of quinoline and the carbonyl oxygen of I227. For the rest of the molecule, the FXa-bound conformation and interaction of **3** with the protein are very similar to those of **2** (Figure 3).

D. RPR131247 (4). The chemical structure of **4** is similar to that of **2** and **3** except for the P1 moiety which is a hydroxybenzamidine. Soaking of FXa crystals in a solution containing compound **4** remained unsuccessful; the structure of **4** was only solved in complex with trypsin (Figure 4). The thienopyridine is located in the S4 pocket. The hydroxybenzamidine overlays quite well with the benzamidine from **1** with a 13° rotation around the amidine which is probably due to the presence of a sulfate ion close to the S1 pocket which is engaged in two H-bonds with the hydroxyl oxygen. The carbonyl oxygen of the pyrrolidinone forms a H-bond with the G219 nitrogen and the sulfonamide does not interact with the protein via any electrostatic interactions. The thienopyridine moiety does not fit in the S4 pocket as well as its equivalent in **2** or **3** with FXa because the pocket is more shallow in trypsin. The thienopyridine is also rotated by 42° when compared with **2** or **3**, and the sulfur atom points toward the protein. The pyridine nitrogen faces out toward the solvent and does not interact with the protein.

Discussion

Compound **1** binds to FXa and trypsin in a canonical fashion typical of a synthetic serine protease inhibitor and appears very similar to that described for the Daiichi FXa inhibitor.⁵ The canonical binding mode is characterized by two main interacting sites (S1 and

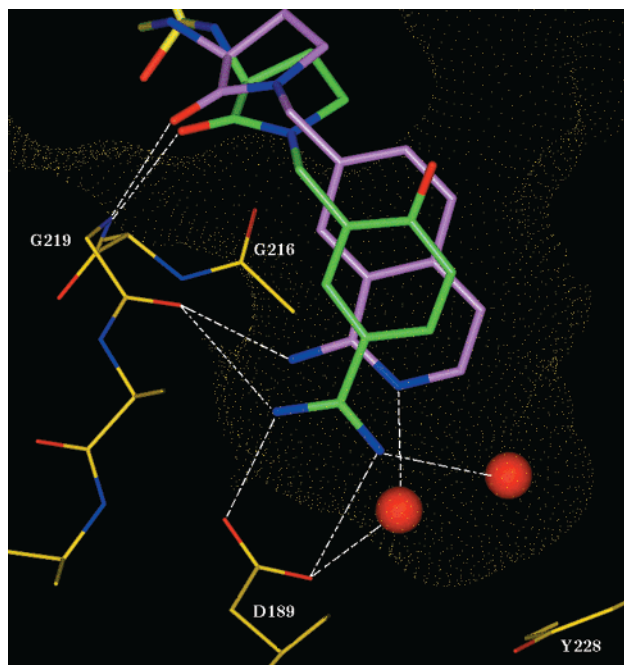


Figure 4. Comparison of **4** bound to trypsin and **3** bound to FXa. Carbon atoms from **3** and **4** are shown in purple and green, respectively. Water molecules from FXa are represented by red balls. The Connolly surface of the S1 pocket is displayed with yellow dots.

S4): formation of a salt bridge between the benzamidine group and D189, hydrophobic contacts with the aromatic ring in the S1 pocket, and hydrophobic interactions in the aryl S4 binding site. However the binding mode of **1** has revealed a new pocket opposite to the S2 subsite which accommodates the ester group of **1**. Interestingly the ester group was initially proposed to interact with the S2 pocket residues. Binding in this cavity seems to play a significant role as removal of the ester function causes a detrimental effect on the binding activity.¹⁰ In

contrast to many thrombin inhibitors¹² for which crystal structures are available, none of the compounds described in this report interact directly with the S2 site. The access to the S2 pocket in FXa is blocked by the side chain of Tyr99, consistent with the preference of glycine for the P2 site. This would suggest that the active site of FXa is capable of accommodating a variety of structurally diverse inhibitors. Similar to other synthetic serine protease inhibitors,¹³ the central β -amino ester or sulfonamidopyrrolidinone scaffolds of **1–4** interact with FXa in a manner which preserves the projection of substituents into the S1 and S4 pockets for productive interactions.

It is known that arylamidine-containing molecules generally display very poor oral absorption¹⁴ and can often be associated with undesirable side effects¹⁵ and thus are unlikely to be successfully developed as oral drugs despite excellent in vitro potencies. The P1 groups of **2** and **3** were designed to replace the benzamidine moiety with a less basic group and consequently were expected to display improved oral bioavailability. The permeability of aminoisoquinoline-containing inhibitors across Caco-2 cell monolayers has been measured and shown to exhibit a 10-fold higher apparent permeability coefficient relative to the corresponding benzamidine-containing compounds.¹¹ Furthermore, the estimated oral bioavailability for **3** is 33% as determined by analysis of ex vivo anti-FXa activity, whereas benzamidine-containing compounds give negligible ex vivo activity. Compounds **2** and **3** were also prepared with the hope that they would make similar interactions with the protein as arylamidine-containing compounds. Conformational restriction of the benzamidine group by a hydrocarbon bridge led to the aminoisoquinoline. Modeling studies indicate that the diaza moiety of aminoisoquinoline from **3** would be optimally positioned to interact with the carboxylate of the S1 subsite.¹¹ The structural data reported here show that this is not the case as no direct contact with D189 is observed. Unlike benzamidine-containing compounds which do not induce the shift of water molecules upon binding, binding of azarene to the carboxylate would require the displacement of a tightly bound solvent molecule (*B*-factor of 28 Å² to compare with the average value of 27 Å² for the protein). Consequently it would appear that the desolvation cost (displacement of this water molecule) is higher than the gain resulting from the increase in van der Waals contact and from the salt bridge formation. One could hypothesize that the location of the P1 group in the S1 subsite is somehow restricted by the interactions of the pyrrolidinone and the thienopyridine with the protein. This assumption is null via two facts. First, the lowest temperature factors for **2** and **3** are found in the P1 group indicative of a very limited flexibility. This would suggest that these contacts in the S1 pocket might correspond to the main driving force of the interaction. This is also observed for benzamidine-containing compounds (**1** and **4**). Second, the structure of **4** bound to trypsin shows that the thienopyridine and pyrrolidinone groups are involved in the same interactions with the protein as those of **2** and **3** when bound to FXa but the hydroxybenzamidine of **4** establishes a salt bridge with D189 in the S1 pocket (Figure 4). It provides evidence that the thienopyridine and the

pyrrolidinone do not prevent a P1 group of similar length from contacting the carboxylate of the S1 subsite. It would suggest that the P1 groups of **2** and **3** do not display the ability to form strong enough interactions with the protein in the lower part of the S1 pocket to counterbalance the desolvation cost. Furthermore despite the 20-fold loss in inhibition potency against FXa, these molecules retain nanomolar range affinity. This underscores that the formation of the salt bridge with D189 is not an absolute requirement for high affinity to FXa. The key interactions in the S1 pocket do not appear to be solely driven by electrostatics. This opens up new prospects in designing FXa inhibitors with high potency and better oral bioavailability containing less basic P1 groups. It has already been reported that certain noncovalent thrombin inhibitors could exhibit high affinity by incorporating nonbasic groups in the P1 position.¹⁶

Conclusion

In summary, we have determined the crystal structure of FXa in complex with potent and selective inhibitors. The benzamidine-containing compound binds in a canonical fashion typical of synthetic serine protease inhibitors. On the contrary, molecules that contain surrogates of the benzamidine group do not make direct hydrogen-bonding interaction with the carboxylate of D189 at the bottom of the S1 pocket. The main interactions involve H-bonding with the G219 carbonyl oxygen in the S1 subsite, hydrophobic contact in the upper part of the S1 pocket, H-bonding with the G219 nitrogen amide, and aromatic contacts in the S4 cleft. The lack of direct electrostatic interaction with D189 suggests that the presence of a highly basic group at the P1 position is not an absolute requirement for maintaining activity. These findings provided new avenues for designing potent and selective FXa inhibitors with good oral bioavailability that do not incorporate strong basic groups in the P1 position. This finding could be applied to the design of compounds targeted toward other serine proteases of pharmacological interest.

Experimental Section

Preparation of the Crystals. Purified human FXa was purchased from Enzyme Research Lab (South Bend, IN). To remove the first 45 amino acids of the light chain (Gla), a 3 mg/mL solution of FXa at pH 8 was treated with α -chymotrypsin (mass ratio 1/100) at room temperature during 150 min. The reaction was stopped with addition of 4-(aminoethyl)-benzenesulfonyl fluoride (Interchim, France) to a final concentration of 1 μ M. Des(1–45)FXa was then purified on a weak cation-exchange resin (Poros 20 CM, P.E. Applied Biosystems) equilibrated in a solution containing 25 mM sodium acetate (pH 5.0). Protein was eluted with a NaCl gradient. For crystallization experiments, the protein was concentrated to 8 mg/mL in 5 mM Mes-NaOH (pH 6.0), 5 mM CaCl₂, 1 μ M **1** on a Vivaspinn ultracentrifugation unit (Vivascience, France). Drops were prepared by mixing 3 μ L of protein solution and 3 μ L of a reservoir solution containing 18–20% PEG 600, 50 mM Mes-NaOH (pH 5.7). Crystals were grown using the hanging drop/vapor diffusion method at 19 °C and they appeared in a few days. A series of seeding cycles was necessary to improve the size and shape of the crystals. Complete details of our efforts to prepare crystals of FXa will be published elsewhere.

Trypsin from bovine pancreas (ethanol precipitate, Sigma ref T8003) was dissolved in 50 mM Mes-NaOH (pH 6.0), 1 mM CaCl₂, 60 mM benzamidine, to a final concentration of 30 mg/mL. Crystals were grown at 19 °C using the hanging drop/

Table 2. Crystal and Diffraction Data of Human FXa with Inhibitors and Trypsin

	FXa/1	FXa/2	FXa/3	trypsin/1	trypsin/4
Crystal Parameters					
space group, cell dimensions (Å)	$P2_12_12_1$, $a = 56.2$, $b = 71.9$, $c = 78.6$	$P2_12_12_1$, $a = 55.6$, $b = 71.6$, $c = 78.7$	$P2_12_12_1$, $a = 56.5$, $b = 72.2$, $c = 77.9$	$P2_12_12_1$, $a = 63.7$, $b = 63.9$, $c = 69.2$	$P2_12_12_1$, $a = 63.4$, $b = 63.8$, $c = 69.3$
resolution (Å)	2.2	2.1	1.9	1.8	1.9
R_{sym}^a (%)	6.1 (23.6)	8.4 (21.7)	4.6 (26.7)	3.9 (13.5)	7.5 (16.5)
completeness ^a (%)	93.9 (91.8)	90.5 (68.6)	99.5 (99.0)	99.7 (97.3)	93.0 (91.7)
no. of reflections, redundancy	15689, 2.7	17166, 3.1	25914, 3.5	26598, 4.3	21256, 3.6
reflections > 5 σ (%)	65.9 (37.1)	77.6 (51.4)	84.95 (65.4)	87.7 (68.3)	85.7 (66.8)
Refinement					
no. of protein atoms (occupancy < 0)	2321	2314	2405	1601	1625
av B -value for protein atoms and ligand atoms (Å ²)	26.1, 27.0	29.8, 35.0	27.0, 31.0	13.7, 17.2	18.7, 12.0
range of data (Å)	20.0–2.2	20.0–2.1	20.0–2.1	8.0–1.8 ^b	15.0–1.9
R -value, R -free (7% of data) (%)	20.8, 26.7	21.6, 26.4	21.1, 26.0	17.9, n/a	17.2, n/a
Weighted rmsd from Ideality					
bond length (Å)	0.007	0.008	0.018	0.007	0.006
bond angle (deg)	1.30	1.25	1.75	1.32	1.36

^a Numbers in parentheses represent statistics in the last shell of data (highest resolution). ^b Trypsin/1 data was restricted to 8.0 Å as no bulk solvent correction was used during crystallographic refinement.

vapor diffusion method and appeared in droplets equilibrated over reservoirs composed of 1.85–1.90 M ammonium sulfate and 50 mM Mes-NaOH (pH 6.0).

X-ray Data Collection and Processing. Crystals were soaked in 50 μ L of mother liquor containing 1–1.5 mM inhibitor and 5–10% dimethylformamide (DMF) for 24–72 h to displace **1** present during the crystallization. Compounds **1–4** were prepared as previously described.^{11,17} For data collection at 95 K the crystals were gradually transferred into a 50- μ L drop composed of the mother liquor supplemented with 1.0–1.5 mM inhibitor, 5–10% DMF and 10% glycerol. Crystals were picked up with a fiber loop and flash-cooled in a stream of gaseous nitrogen at 95 K. The X-ray intensity data were collected on DIP2000 imaging plate (Mac Sciences, Japan) mounted on a FR591 rotating anode (Nonius, The Netherlands), operated at 50 kV, 90 mA. Data processing and scaling were carried out using DENZO and SCALEPACK.¹⁸ Crystal data are presented in Table 2.

Structure Solution and Crystallographic Refinement. The structures were solved by molecular replacement. The search model was made from the coordinates of the refined structure of unliganded FXa.⁴ Energy-restrained least-squares refinement was carried out using X-PLOR.¹⁹ In the final stages of refinement, individual temperature factors were also refined. Solvent molecules were included if they were on sites of difference electron density with values above 2.5 σ and if they were within 3.5 Å of the protein molecule or a water molecule. All non-glycine residues fall within the energetically favorable regions (84% in the most favored regions and 15.7% in the additional allowed regions). All atoms of the inhibitors and of FXa lie in well-defined electron density except the EGF1 domain which was not visible. The statistics of the crystallographic refinement are shown in Table 2. Atomic coordinates have been deposited with the Protein Data Bank (1ezq, 1f0s, 1f0u, 1f0t, 1f0r).

Acknowledgment. Michael Myers is gratefully acknowledged for critically reading the manuscript and Michael Ashton for constant support.

References

- Prager, N. A.; Abendschein, D. R.; McKenzie, C. R.; Eisenberg, P. R. Role of thrombin compared with factor Xa in the procoagulant activity of whole blood clots. *Circulation* **1995**, *92*, 962–967.
- Kaiser, B. Thrombin and factor Xa inhibitors. *Drugs Future* **1998**, *23*, 423–436.
- Weitz, J. I. Low molecular weight heparins. *N. Engl. J. Med.* **1997**, *337*, 688–698.
- Padmanabhan, K.; Padmanabhan, K. P.; Tulinsky, A.; Park, C. H.; Bode, W.; Huber, R.; Blankenship, D. T.; Cardin, A. D.; Kisiel, W. Structure of human des(1–45) factor Xa at 2.2 Å. *J. Mol. Biol.* **1993**, *232*, 947–966.
- Brandstetter, H.; Kühne, A.; Bode, W.; Huber, R.; von der Saal, W.; Wirthensohn, K.; Engh, R. A. X-ray structure of the active site-inhibited clotting factor Xa. *J. Biol. Chem.* **1996**, *271*, 29988–29992.
- Kamata, K.; Kawamoto, H.; Honma, T.; Iwama, T.; Kim, S.-H. Structural basis for chemical inhibition of human blood coagulation factor Xa. *Proc. Natl. Acad. Sci. U.S.A.* **1998**, *95*, 6630–6635.
- Stubbs, M.; Bode, W. Crystal structures of thrombin and thrombin complexes as a framework for antithrombotic drug design. *Perspect. Drug Discovery Des.* **1994**, *1*, 431–452.
- Whitlow, M.; Arnaiz, D. O.; Buckman, B. O.; Davey, D. D.; Griedel, B.; Guilford, W. J.; Koovakkat, S. K.; Liang, A.; Mohan, R.; Phillips, G. B.; Seto, M.; Shaw, K. J.; Xu, W.; Zhao, Z.; Light, D. R.; Morissey, M. M. Crystallographic analysis of potent and selective factor Xa inhibitors complexed to bovine trypsin. *Acta Crystallogr. Sect. D* **1999**, *55*, 1395–1404.
- Stubbs, M.; Huber, R.; Bode, W. Crystal structures of factor Xa specific inhibitors in complex with trypsin: structural grounds for inhibition of factor Xa and selectivity against thrombin. *FEBS Lett.* **1995**, *375*, 103–107.
- Klein, S. I.; Czekaj, M.; Gardner, C. J.; Guertin, K. R.; Cheney, D. L.; Spada, A. P.; Bolton, S. A.; Brown, K.; Colussi, D. J.; Heran, C. L.; Morgan, S. R.; Leadley, R. J.; Dunwiddie, C. T.; Perrone, M. H.; Chu, V. Identification and initial structure–activity relationships of a novel class of nonpeptide inhibitors of blood coagulation factor Xa. *J. Med. Chem.* **1998**, *41*, 437–450.
- Choi-Sledeski, Y. M.; Becker, M. R.; Green, D. M.; Davis, R.; Ewing, W. R.; Mason, H. J.; Ly, C.; Spada, A.; Liang, G.; Cheney, D.; Barton, J.; Chu, V.; Brown, K.; Colussi, D.; Bentley, R.; Leadley, R.; Dunwiddie, C.; Pauls, H. W. Aminoisoquinolines: design and synthesis of an orally active benzamidin isostere for the inhibition of factor Xa. *Bioorg. Med. Chem. Lett.* **1999**, *9*, 2539–2544.
- Sanderson, P. E. J.; Naylor-Olsen, A. M. Thrombin inhibitor design. *Curr. Med. Chem.* **1998**, *5*, 289–304.
- Leung, D.; Abbenante, G.; Fairlie, D. P. Protease inhibitors: current status and future prospects. *J. Med. Chem.* **2000**, *43*, 305–401.
- Rewinkel, J. B. M.; Lucas, H.; Smit, M. J.; Noach, A. B. J.; van Dinther, T. G.; Rood, A. M. M.; Jenneboer, A. J. S. M.; van Boeckel, C. A. A. Design, synthesis and testing of amino-bicycloaryl based orally bioavailable thrombin inhibitor. *Bioorg. Med. Chem. Lett.* **1999**, *9*, 2837–2842.
- Hauptmann, J. Pharmacology of benzamidin-type thrombin inhibitors. *Folia Haematol.* **1982**, *109*, 89–97.
- Tucker, T. J.; Brady, S. F.; Lumma, W. C.; Lewis, S. D.; Gardell, S. J.; Naylor-Olsen, A. L.; Yan, Y.; Sisko, J. T.; Stauffer, K. J.; Lucas, B. J.; Lynch, J. J.; Cook, J. J.; Stranieri, M. T.; Holahan,

- M. A.; Lyle, E. A.; Baskin, E. P.; Chen, I. W.; Dancheck, K. B.; Krueger, J. A.; Cooper, C. M. 1 Vacca, J. Design and synthesis of a series of potent and orally bioavailable noncovalent thrombin inhibitors that utilize nonbasic groups in the P1 position. *J. Med. Chem.* **1998**, *41*, 3210–3219.
- (17) Choi-Sledeski, Y. M.; McGarry, D. G.; Green, D. M.; Mason, H. J.; Becker, M. R.; Davis, R.; Ewing, W. R.; Dankulich, W. P.; Manetta, V. E.; Morris, R. L.; Spada, A.; Cheney, D.; Brown, K.; Colussi, D. J.; Chu, V.; Heran, C. L.; Morgan, S. R.; Bentley, R.; Leadley, R.; Maignan, S.; Guilloteau, J.-P.; Dunwiddie, C.; Pauls, H. W. Sulfonamidopyrrolidinone factor Xa inhibitors: potency and selectivity enhancements via P-1 and P-4 optimization. *J. Med. Chem.* **1999**, *42*, 3572–3587.
- (18) Otwinowski Z.; Minor, W. Processing of X-ray diffraction data collected in oscillation mode. *Methods Enzymol.* **1997**, *276*, 307–326.
- (19) Brünger, A. T. *X-PLOR Version 3.1: A System for X-ray Crystallography and NMR*; Yale University Press: New Haven, CT, 1992.
- (20) Bostwick, J. S.; Bentley, R.; Morgan, S.; Brown, K.; Chu, V.; Ewing, W. R.; Spada, A.; Pauls, H.; Perrone, M.; Dunwiddie, C. T.; Leadley, R. J. RPR120844, a novel specific inhibitor of coagulation factor Xa inhibits venous thrombosis in the rabbit. *Thromb. Haemost.* **1999**, *81*, 157–160.

JM000940U